

Effects of Adding Noise to Circuit Model and Numerical Model of Spontaneous Otoacoustic Emissions

Lucy Feng¹ and Carey Witkov[#]

¹The Harker School, San Jose, CA, USA

[#]Advisor

ABSTRACT

Spontaneous otoacoustic emissions have long been modeled using self-excited, nonlinear oscillators. The van der Pol oscillator is a common choice, as many of its properties reflect those of SOAEs: both can begin oscillation in the absence of a direct stimulus, both have narrow frequency bands, and both become stable over time, to name a few. Yet such an idealized equation cannot have a one-to-one correspondence with SOAEs in all factors. Many previously used mathematical and circuit models lack the addition of noise to more accurately show how real world SOAEs operate in an organism's ear, where noise from the environment is almost entirely unavoidable. The inclusion of uniformly distributed noise in both numerical and circuit models of the van der Pol oscillator was studied to determine whether these models can still accurately explicate SOAEs when modified to be more realistic. In both cases, both models retained the attributes of real world SOAEs despite the addition of noise, allowing them to serve as more useful and accurate models of the phenomenon.

Introduction

While most people think of the ear as a receptor for auditory signals, many are unaware of its ability to produce sounds, which are referred to as otoacoustic emissions. These emissions are produced in the cochlea as a by-product of an active amplification process in the cochlea. OAEs can be categorized into three major types: evoked OAEs, distortion product OAEs (DPOAEs), and spontaneous OAEs (SOAEs), which are the focus of this study's research. Unlike the other two types of OAEs, spontaneous otoacoustic emissions do not require a stimulus to occur.

Within the inner ear sits the cochlea, a snail shell shaped structure responsible for translating vibrations of the eardrum into electrical signals. Vibrations in the basilar membrane, which separates the two chambers of fluid inside the cochlea, cause the outer hair cells also within the cochlea to lengthen and shorten, which mechanically amplifies softer sounds that are converted into electrical pulses by the inner hair cells. Conversely, the outer hair cells change their lengths when they detect electrical signals, creating a feedback loop analogous to that of a microphone and speaker when the two get too close or the gain is turned up too high, producing a shrill tone.

SOAEs are in fact not limited to cochlear ears. Any nonlinear active process, such as the vibrations of the membrane (tympanum) in tympanal hearing, will produce SOAEs. In other words, any ear that involves nonlinear oscillations of some structure may spontaneously produce sounds, regardless of the presence of a cochlea.

There are several defining characteristics that can be found in SOAE lines: narrow bandwidth, asymmetry, and stability over time. A narrow bandwidth indicates the purity of tone of SOAEs, that the sounds produced in SOAEs are more like a single note than a muddy smattering of noise. These pure tones present as peaks on frequency distribution plots and have asymmetrical Lorentzian distributions, specifically that the center of the peak is shifted more towards the higher frequency end. Some have suggested using SOAEs as an

alternative to fingerprints for identification, as SOAE frequencies are both extremely stable and unique to the individual.

The stability of SOAEs is due to the fact that SOAEs behave like limit cycle oscillators. A limit cycle oscillator does not require a driving force, meaning it can be started simply with noise. Regardless of what the initial conditions of the oscillator are, the pattern of oscillation will eventually stabilize to a certain amplitude. The van der Pol oscillator is the simplest nonlinear oscillator that exhibits a limit cycle, another reason it was chosen as the baseline for modeling SOAEs.

Another characteristic of the SOAE nonlinear oscillator is the production of odd harmonic frequencies in its frequency spectrum. Due to the complexity of the human cochlea, it is unlikely that human SOAEs will produce a spectrum of only odd harmonic frequencies, as many factors unrelated to SOAEs may influence the spectrum. A less complex organism however, such as an insect, may produce the more simplified spectrum of solely odd harmonics as seen in the numerical simulation of the van der Pol equation. A paper by Natasha Mhatre and Daniel Robert analyzed data of cricket SOAEs. Specifically, their Figure 1c, which traces the frequency spectrum of 12 subjects, shows prominent odd harmonics at 1, 3, and 5 kHz, a result that reflects the frequency spectrum from the our mathematical model of SOAEs exceptionally well.

Background

Astrophysicist Thomas Gold first proposed (1948) that the ear generates sounds based on its extreme amplification and the known oscillations that result from feedback amplifiers. However, unable to detect the sounds generated by the ear using the equipment he had, the discovery was not made until 1978 when David Kemp succeeded. Soon thereafter, detection of otoacoustic emissions became the standard method for assessing hearing in newborns. However, in its most basic form, a Van der Pol oscillator cannot perfectly reflect data taken from real world SOAE analysis, which include the many nuances of the imperfect world. Thus, many efforts have been made to extend the capabilities of a simple Van der Pol oscillator so a more accurate representation of spontaneous otoacoustic emissions can be achieved. A study modeling lizard SOAEs found that the addition of Gaussian (normally distributed) noise created new peaks in certain frequencies while also making the tones of the resonant frequencies less pure, as the range of each peak in the spectrum was widened.

Research Question

Our specific question for targeted research was as follows: how does adding uniformly distributed noise to both the mathematical and circuit models of SOAEs affect their accuracy with regards to real world SOAEs?

Methods

Circuit Simulation

We utilized the circuit simulation to explore SOAEs from a hands-on perspective as an alternative to real world data from SOAEs.

The circuit simulation we used was created by Paul Falstad, who has created several other simulations with a significantly wider range of capabilities than those typically found in a high school classroom. For this study, his circuit simulator, which includes circuit elements of almost every variety, was used to tweak and refine a simple harmonic oscillator to eventually arrive at a circuit for the van der Pol oscillator. Several variations of van der Pol circuits exist, though in nearly all of them, both a capacitor and an inductor are utilized. We first settled on a seven element LC oscillator made up of a noise generator, three resistors, a capacitor, an

inductor, and a tunnel diode, but found that it was not nonlinear enough to describe SOAEs. Specifically, the log spectrum of frequencies for the LC oscillator showed peaks at both the odd and even multiples of the fundamental frequency instead of just the odd multiples, which was what we saw in the cricket SOAE data. Therefore, we turned to the relaxation oscillator instead, as it was much more nonlinear and produced only the odd harmonics in its log spectrum plot.

Our final circuit model consisted of five electrical elements: a noise generator, two resistors, an inductor, and a tunnel diode. The noise generator acts as both the voltage source and the source of uniformly distributed, or Gaussian, noise in the system. Within our model, the DC offset (essentially the voltage) was set to 1.5 V and maximum voltage for noise varied between 0 and 600 mV to test for a range of amounts of noise. Two resistors were added to the circuit, one of which was connected in series with the voltage source and the other was connected to a ground and in parallel to the noise generator. Next added in parallel and attached to a ground was an inductor as a means of storing the magnetic energy of the system. Finally, the self-exciting nature of the circuit is due to the tunnel diode, a type of diode that exhibits the quantum qualities of “tunneling” to allow for what is essentially negative resistance. Diodes act as a sort of one way switch, allowing current to flow in one direction but not the other, and they require a minimum threshold voltage to operate properly. A tunnel diode has the additional property that when a voltage within a certain range is applied, an increasing voltage induces a decreasing current, resulting in the system oscillating without an external force or voltage. Since resistance is the quotient of voltage and current, the negative slope of the tunnel diode's Voltage vs Current plot represents a negative resistance that cancels circuit resistance, facilitating self-oscillation. An image of the circuit used is shown below.

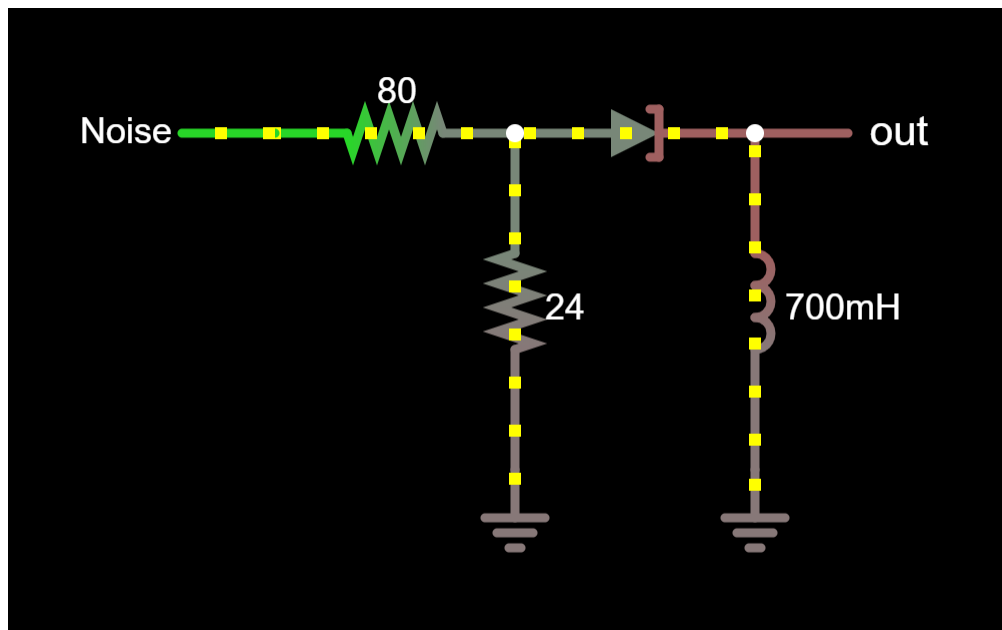


Figure 1. Circuit model configuration using Falstad Circuit Simulator. The resistances of the resistors are shown in ohms.

Numerical Simulation

The van der Pol equation is a nonlinear differential equation. For algebraic equations, the solution is a number. For a differential equation, the solution is a function. The vast majority of nonlinear differential equations however do not have closed form solutions. Therefore, they can only be solved numerically with step-by-step values,

making nonlinear differential equations great to be solved via a spreadsheet, which can crunch a large amount of numbers.

One commonly used technique of solving nonlinear differential equations is to employ the Euler method, which essentially consists of plugging increasing values of time into update equations and plotting the numerical answers to those results. While the Euler method is simple and straightforward, using large time steps can lead to a lot of deviation. In the case of the Euler method, which is a first order method, the error introduced in each step is proportional to the size of each step squared, and thus a larger step size will generate more errors. In 1980, by a pure stroke of luck, a high schooler exchanged the position update statement and the velocity update statement in her computer code for the Euler method, believing she had made an error when her solution began to diverge after 14 iterations. This simple switch of using the new velocity (that is, the velocity that would usually be calculated in the next step of the Euler method) instead of the old one in the position update statement produced results that were significantly more stable for a longer period of time. Later named the Euler-Cromer method, this was the method implemented in our spreadsheet.

Equations Utilized in the Excel Spreadsheet

The van der Pol equation looks as follows:

$$a - \mu(1 - x^2)v + \omega^2x = 0,$$

where v is the rate of change of position with respect to time (also known as velocity) and a is the rate of change of velocity with respect to time (also known as acceleration). Position is represented by the variable x . ω controls the frequency, and μ controls the amount of damping: a larger value of μ indicates a more nonlinear equation. The equation for velocity is $v = \frac{\Delta x}{\Delta t}$, where Δx is defined as $x_{new} - x_{old}$. Rearranging the equation results in

$$x_{new} = x_{old} + v\Delta t.$$

For the Euler method, the v in the above equation would be the old velocity, but in the Euler-Cromer method, that would be new velocity. Acceleration can be described as $a = \frac{\Delta v}{\Delta t}$ and can be rearranged to form

$$v_{new} = v_{old} + a\Delta t,$$

giving us the update statements for both position and velocity. The update equation for velocity, however, requires the value of the acceleration, which can be defined as

$$a = \mu(1 - x^2)v - \omega^2x$$

by rearranging the van der Pol equation.

The above equations were utilized in the Excel spreadsheet to create the different columns of values later used to create the plots. The first column of the spreadsheet contained increasing values for the time, with the difference between cells being 0.05 seconds. A smaller time increment had to be chosen to allow for a smoother and more accurate plot, as too large a time interval would result in more deviation. The fast Fourier transform (FFT) requires that the number of samples be a power of 2. 1024 samples meet that requirement and provides sufficient frequency resolution as the Nyquist sampling theorem limits frequency resolution to no finer than half the sampling rate. Column E held the values for the velocity, where the initial velocity was set to 0.100, and each subsequent cell was calculated with the velocity update equation.

To obtain the FFT frequency, FFT magnitude, and FFT complex values, the Fourier transform function of the Excel spreadsheet was utilized. To put into simple terms, the Fourier analysis breaks a whole down into its component frequencies, like a prism would break white light down into its component frequencies, which are the different colors of a rainbow.

Results

The following figures were taken from the circuit and numerical models and were analyzed for narrow bandwidth, asymmetry, and stability over time.

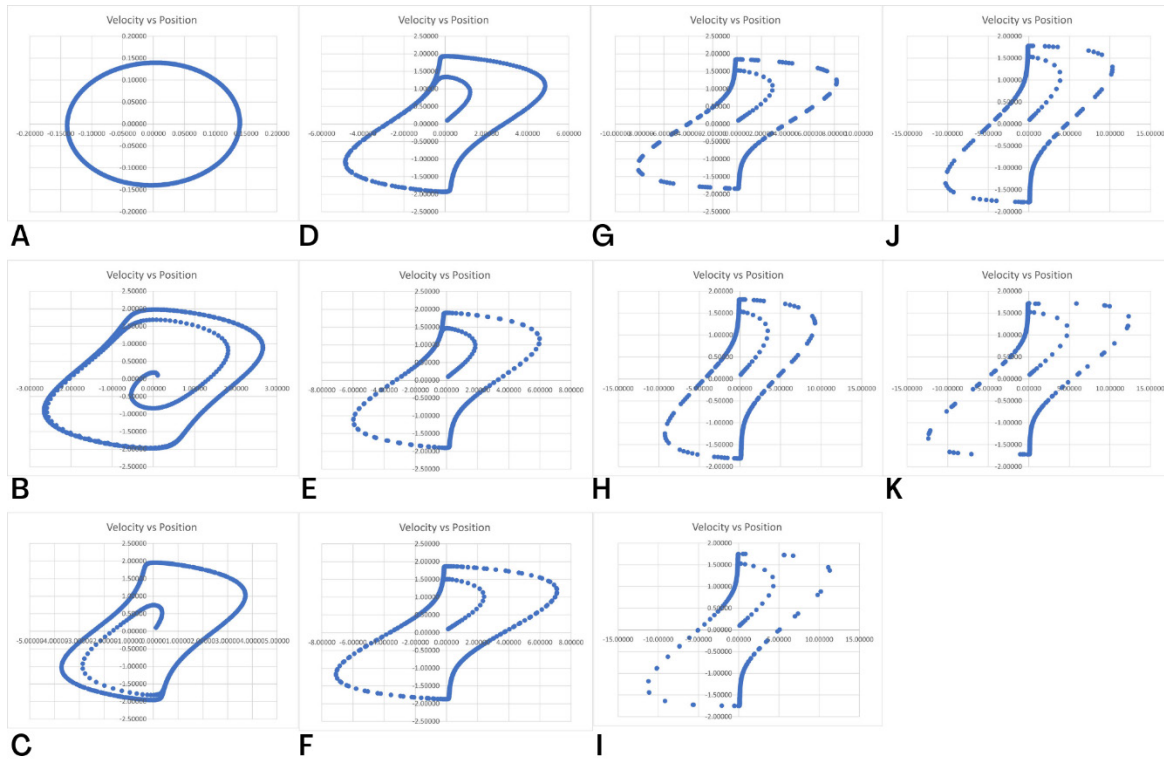


Figure 2. Velocity vs. Position plots from the numerical model on Excel Spreadsheet. Figure 2A shows the plot when $\mu = 0$, 2B when $\mu = 1$, 2C when $\mu = 2$, 2D when $\mu = 3$, 2E when $\mu = 4$, 2F when $\mu = 5$, 2G when $\mu = 6$, 2H when $\mu = 7$, 2I when $\mu = 8$, 2J when $\mu = 9$, and 2K when $\mu = 10$. Starting in Figure 2B, the limit cycle becomes apparent as the data points begin at the origin and fall into the parallelogram-like shape cycle. As μ was increased, the points fell into the limit cycle quicker. Regardless of the initial starting point on the phase diagram, the solution traced out by the vector field (not visible) will eventually stabilize within the limit cycle.

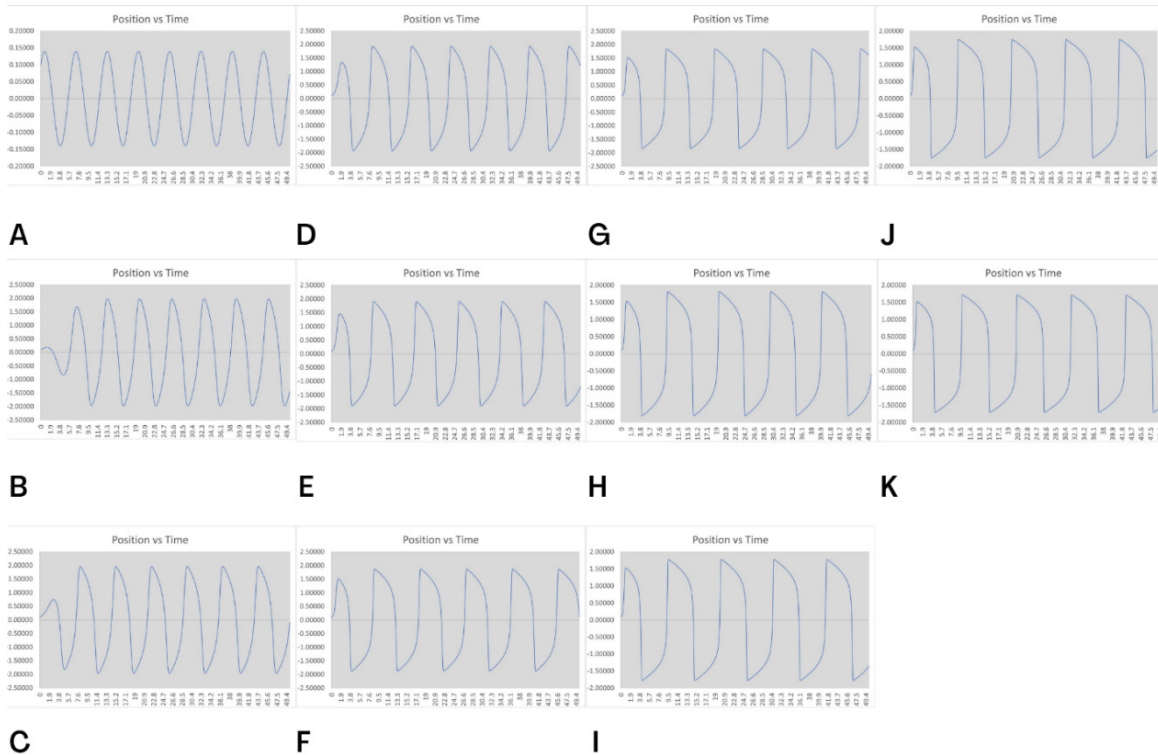


Figure 3. Position vs. Time plots from the numerical model on Excel Spreadsheet. Figure 3A shows the plot when $\mu = 0$, 3B when $\mu = 1$, 3C when $\mu = 2$, 3D when $\mu = 3$, 3E when $\mu = 4$, 3F when $\mu = 5$, 3G when $\mu = 6$, 3H when $\mu = 7$, 3I when $\mu = 8$, 3J when $\mu = 9$, and 3K when $\mu = 10$. As μ was increased to increase the damping, the plots began to deviate from a sinusoidal shape and into asymmetrical curves, a display of the fast/slow dynamic system. Vertical sections of the plots indicate faster velocities characteristic of non-linear oscillation.

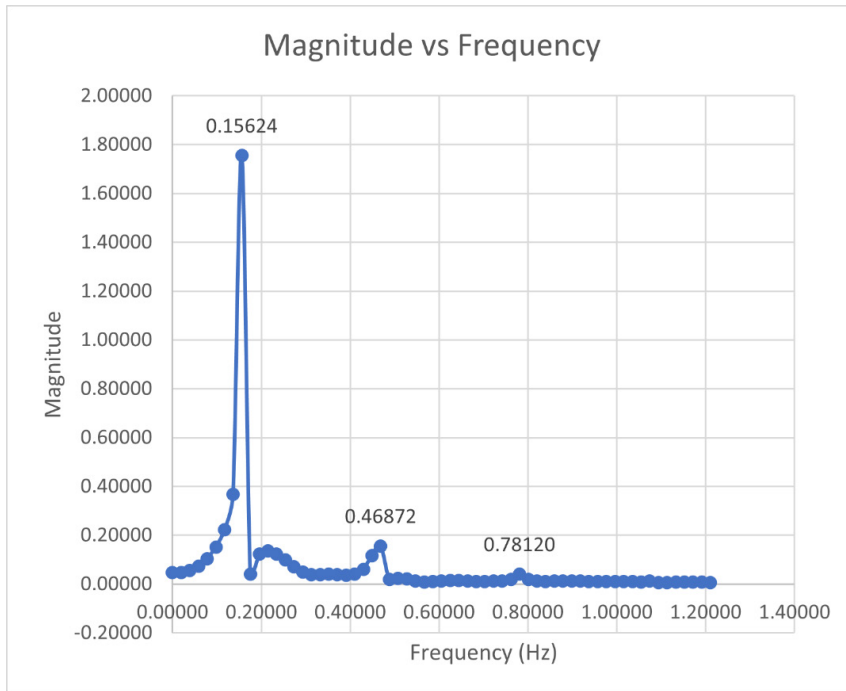


Figure 4. Magnitude vs. Frequency plot taken from numerical model on Excel Spreadsheet. The fundamental frequency occurs at 0.15624 Hz, and successive peaks occur at the 3rd and 5th harmonics of the fundamental frequency.

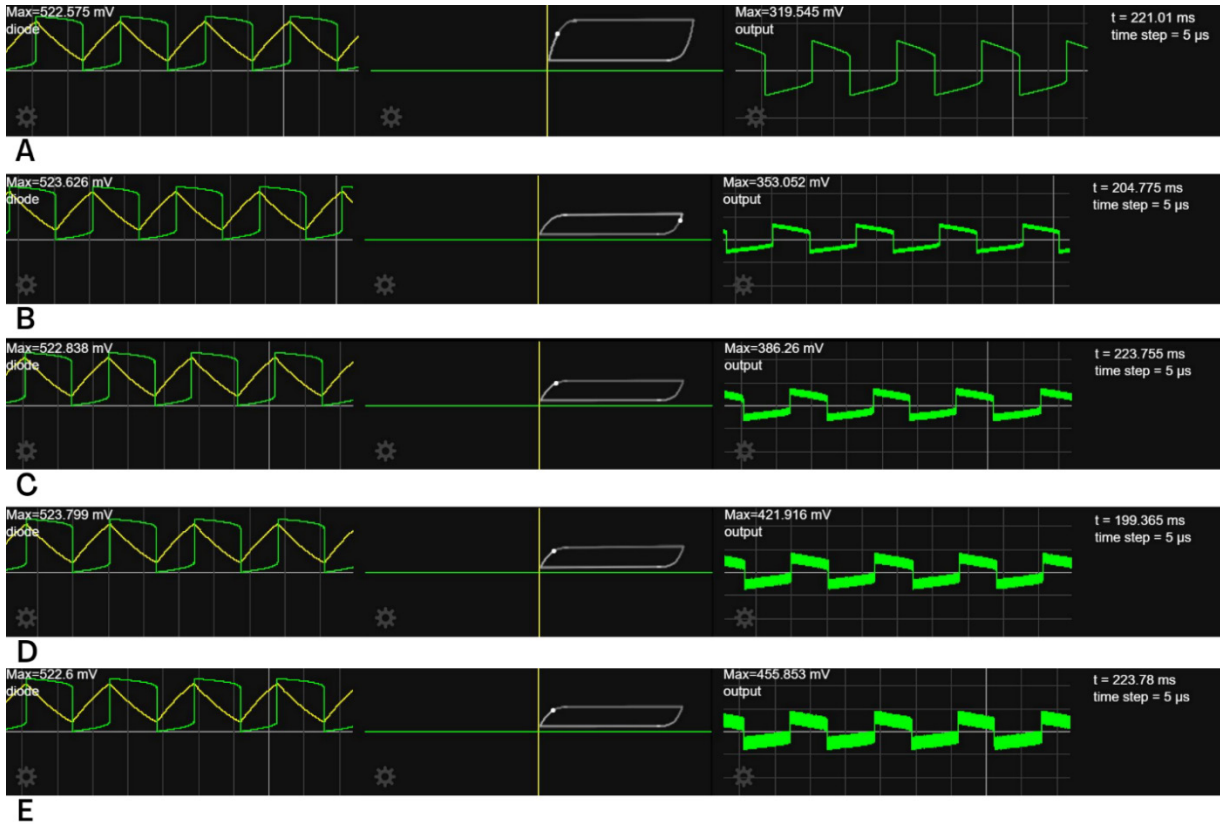


Figure 5. Plots taken from the Falstad Circuit Simulator. (From left to right) Current vs. Time and Voltage vs. Time plot for the tunnel diode, Current vs. Voltage plot for the tunnel diode, and Voltage vs. Time plot for the output. Figure 5A shows plots when the noise has a maximum voltage of 0 mV, Figure 5B when the voltage of noise is 150 mV, Figure 5C when voltage of noise is 300 mV, Figure 5D when the voltage of noise is 450 mV, and Figure 5E when the voltage of noise is 600 mV. As noise was increased, the Voltage vs. Time plot fluctuated but maintained a nonlinear shape as seen in the numerical model.

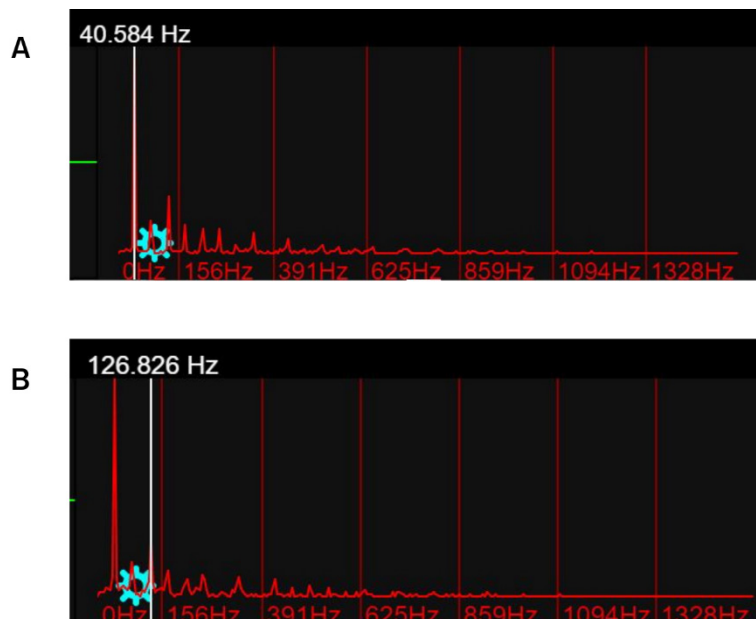


Figure 6. Magnitude vs. Frequency plots taken from the Falstad Circuit Simulation when voltage of noise is 600 mV. The highest peaks occur at roughly 40 Hz, the fundamental frequency, and 120 Hz, the 3rd harmonic of the fundamental, following in line with the expected odd harmonics found in SOAEs.

Analysis

Plots of both the circuit model and mathematical model reflect the three major characteristics of SOAEs: narrow bandwidth, asymmetry, and stability over time. Peaks in the Magnitude vs. Frequency plots for both models are very narrow, resembling more a point than a plateau. In correspondence to the asymmetry of SOAEs, these peaks all lean more to the left than to the right, as in, the maximum of each peak is closer to the left side than the right side (this is much more apparent in the spreadsheet model's plots but exists as well in the spectrums for the circuit model). In addition, Figure 4 displays the fundamental frequency at 0.15624 Hz as well as smaller peaks of decreasing size at odd multiples of that main peak frequency (0.46872 Hz, 0.78120 Hz). The same is true for the frequency spectrums in the circuit model, though the numbers are less perfectly rounded because the plot is not static.

As the noise was increased in the circuit model, the Voltage vs. Time plots in Figure 5 became less regular, having more fluctuations that when close together looks like the thickness of the line has increased. This phenomenon is not necessarily germane to modeling SOAEs however, as in nearly any circuit the voltage source becomes less stable with the addition of noise.

Within the spreadsheet, as μ was increased (which determines the nonlinearity of the equation), the Position vs. Time plot began to deviate from a standard sinusoidal shape, instead more closely resembling the Voltage vs. Time plot taken from the circuit simulation. In our case, Position refers to the same thing as Voltage, since in both cases they are replacing the x variable in the Van der Pol equation. The effect of increasing μ on the Velocity vs. Position plot (or the phase plot) results in the following interesting changes. When μ is set to a value greater than zero, the phase plot begins to display characteristics pertaining to a limit cycle oscillator. As time increases, the line of the plot falls into an irregularly elliptical shape and remains on this perimeter forever. For greater values of μ , the shape of the limit cycle was less and less regular, but the line of the plot falls into the limit cycle earlier. Though our spreadsheet only tests for one set of initial conditions, because we know the Van der Pol oscillator is a limit cycle oscillator, this same phenomenon would occur regardless of the starting point for the plot. The plot therefore serves as proof for the stability of our mathematical model over time, another prominent feature of SOAEs. The stability for our circuit model is less easily discerned, as the simulation is animated to be not static, but after the simulation ran for about a minute, the frequency spectrum stabilized enough so the fundamental frequencies and odd harmonics could be distinguished from the constantly fluctuating noise.

Conclusion

Our data showed that despite the addition of uniformly distributed noise to both the circuit and mathematical models, they retained their ability to accurately reflect real world SOAEs, specifically those of lower organisms like crickets. Specifically, the distinguishing properties of SOAEs, odd harmonics, narrow bandwidth, and waveform asymmetry, were all captured by van der Pol oscillator circuit and numerical simulations. In general, the confirmation that these two representations of Van der Pol oscillators (circuit and numerical), continue to effectively model SOAEs even with the addition of noise, should prove helpful to SOAE researchers in forming hypotheses and designing experiments.

Discussion

In recent years, researchers have been looking into the real world applications of SOAE properties. As mentioned briefly in the introduction, one such application is in biometrics, to use the stable frequencies of an individual's SOAEs as a sort of fingerprint identification. The spreadsheet model we tested in this study could be useful in developing software that distinguishes between random noise and the true frequencies as generated by SOAEs. Additionally, studies have revealed a relationship between Idiopathic Sudden Deafness and the lack of presence or strength of SOAEs in subjects, specifically that as hearing returned to the subjects, their SOAEs could be detected once more. The models tested in this study could be utilized to develop possible treatments for hearing loss by manipulation of SOAEs in the human ear. In general, the results as detailed in the paper serve as a baseline to which SOAE data from experimentation can be compared and open the door to both hardware and software development that exploit the key properties of SOAEs.

Acknowledgments

I would like to express my deepest gratitude to Dr. Carey Witkov of Harvard University, my academic mentor, for providing crucial guidance on the topic of SOAEs and the Van der Pol oscillator. His knowledge and aid throughout the research process have been invaluable. I would additionally like to thank Omar Hayat, my teaching assistant, for his constant support during the editing and proofreading process.

References

Cromer, Alan. "Stable solutions using the Euler approximation." *American Journal of Physics* 49(5), pp. 455–459, (1981). doi: 10.1119/1.12478.

Duifhuis, Hendrikus. "Hopf-Bifurcations and Van der Pol Oscillator Models of the Mammalian Cochlea." *AIP Conference Proceedings* 1403, pp. 199-205, (2011). doi: 10.1063/1.3658086.

Gorga, Michael P. et al. "A comparison of transient-evoked and distortion product otoacoustic emissions in normal-hearing and hearing-impaired subjects", *The Journal of the Acoustical Society of America* 94, pp. 2639-2648 (1993) doi: 10.1121/1.407348.

Grabham, Neil et al. "An Evaluation of Otoacoustic Emissions as a Biometric," in *IEEE Transactions on Information Forensics and Security*, vol. 8, no. 1, pp. 174-183, Jan. 2013, doi: 10.1109/TIFS.2012.2228854.

Long, Glenis et al. "Modeling synchronization and suppression of spontaneous otoacoustic emissions using Van der Pol oscillators: Effects of aspirin administration." *The Journal of the Acoustical Society of America* 89, pp. 1201-12, (1991).

Mhatre, Natasha & Robert, Daniel. "A Tympanal Insect Ear Exploits a Critical Oscillator for Active Amplification and Tuning." *Current Biology*, pp. 1952-1957, (2013). doi: 10.1016/j.cub.2013.08.028.

Murphy, W. J. et al. "Relaxation dynamics of spontaneous otoacoustic emissions perturbed by external tones. I. Response to pulsed single-tone suppressors." *The Journal of the Acoustical Society of America* 97, pp. 3702-3710, (1995). doi: 10.1121/1.412387.

Nakamura, M. et al. "Changes in Otoacoustic Emissions in Patients with Idiopathic Sudden Deafness." *Audiology*, 36:3, pp. 121-135, (1997). DOI: 10.3109/00206099709071966.

Talmadge, Carrick L. et al. "Are spontaneous otoacoustic emissions generated by self-sustained cochlear oscillators?" *J. Acoust. Soc. Am.* 89, pp. 2391–2399, (1991). doi: 10.1121/1.400958.

Talmadge, Carrick L. et al. "Quantitative Evaluation of Limit-Cycle Oscillator Models of Spontaneous Otoacoustic Emissions." doi: 10.1007/978-1-4757-4341-8_29.

Zurek, P. M. "Acoustic emissions from the ear: a summary of results from humans and animals." *The Journal of the Acoustical Society of America*, 78(1 Pt 2), pp. 340–344, (1985). doi: 10.1121/1.392496.